Composites & nanocomposites

Modeling the effect of oxidation on the residual tensile strength of SiC/C/SiC minicomposites in stressed oxidizing environments

Xihui Chen[2] , Zhigang Sun[2,3], Hongyu Li[2], Yingdong Song[1,2,3,*], and Xuming Niu[2]

[1] State Key Laboratory of Mechanics and Control Mechanical Structures, Nanjing University of Aeronautics and Astronautics, Nanjing 210016, People's Republic of China
[2] Jiangsu Province Key Laboratory of Aerospace Power System, College of Energy and Power Engineering, Nanjing University of Aeronautics and Astronautics, Nanjing 210016, People's Republic of China
[3] Key Laboratory of Aero-engine Thermal Environment and Structure, Ministry of Industry and Information Technology, Nanjing 210016, People's Republic of China

ABSTRACT

A micromechanics model is presented to predict the residual tensile strength of SiC/C/SiC minicomposites within the temperature range of 900–1300 °C in stressed oxidizing environments. The model is based on a new oxidation kinetics model of 1D-SiC/C/SiC composites, which gives the silica thickness profiles along the matrix cracks and the annular pores, the length of carbon interface consumed by oxidation. Based upon the length of carbon interface consumed by oxidation and the silica thickness profile on the fiber surface, the fiber stress distribution and the residual tensile strength of fibers are calculated. The probability of failure of the fibers is obtained considering the fiber stress distribution and residual tensile strength of fibers. Combining the probability of failure of the fibers with the matrix cracking model, the residual tensile strength is calculated. The predicted values agree well with the residual strength derived from the oxidation experiments. This indicates the reliability of the analytical model.

Introduction

Silicon carbide fibers–reinforced silicon carbide matrix (SiC_f/SiC) composites exhibit a variety of performance advantages for use as high-temperature structural materials in aerospace engine systems due to their high specific strength/modulus, oxidation resistance and stability at high temperatures [1–4]. PyroCarbon (PyC), because of its strong anisotropy in properties and microstructure, as well as the fact that it serves to protect the fibers during processing, was

thought to be the best interface material for SiC/SiC in terms of its mechanical behavior [5–7].

Matrix cracking occurs during initial application of a tensile stress [8]. The cracks in the matrix allow the ingress of oxidizing species (oxygen) into the interior of SiC/C/SiC composites for oxygen diffusing in oxidizing atmosphere [9]. The carbon interface is readily oxidized at temperatures as low as 500 °C with formation of gaseous oxides [10]. The SiC fibers and matrix may undergo passive oxidation at high temperature (> 900 °C) in the atmosphere of high oxygen pressures with formation of gaseous and solid oxides [11].

The oxidation of carbon interface creates tubular channels between the SiC fibers and matrix [12, 13], whose silicon carbide surfaces also oxidize, leading to the creation of silica. This oxidation mechanism (sometimes called "pipeline oxidation") has been already observed in 1D-SiC/C/SiC composites [14]. For longer oxidation times and/or higher temperatures, the silica created on the surfaces exposed to oxygen tends to fill up the tubular channels and then to stop the diffusion of oxygen and the oxidation of carbon [12]. Meanwhile, the oxidation of these constituents of SiC/C/SiC composites leads to the change in weight [15, 16]. Ludovic Filipuzzi et al. [10] have already modeled the oxidation kinetics of 1D-SiC/C/SiC composites under nonstress condition in dry oxygen environment and given the changes in oxygen concentration profile along the annular pore, the variations of carbon interface length consumed by oxidation, the variations of the relative weight change of the composite. The variation in carbon interface length was validated by the resistance measurement of the composite, and the variation in the relative weight change was validated by the TGA under flowing dry oxygen [14]. However, the model did not take into account the fact that the matrix cracks are main channels of oxygen diffusion in stressed oxidizing environments. Although the sealing of annular pore of the composite with a thin carbon interface was reported, the model could not take into the closure of matrix cracks due to reaction with walls or the resulting change in the crack width.

On the other hand, the oxidation of carbon interface and SiC fibers causes the degradation of fiber/matrix interface and fiber's properties and changes the stress distribution in the bulk composite system [17, 18], which leads to a severe decrease in ultimate strength and toughness of the composite

[19]. Morscher et al. [20] found that severe degradation in tensile strength of SiC/C/SiC minicomposites in air oxidizing environment at temperatures in the range of 700–950 °C was due to degradation of the SiC fiber properties. When exposed to oxidizing environments at intermediate temperatures (700–900 °C), they can exhibit severe embrittlement and fracture at stresses that are well below their ultimate strength in the pristine state [21–24]. This embrittlement is absent (or proceeds slowly) at both lower and higher temperatures [25]. Pailler et al. [9] proposed a micromechanics-based model of the thermomechanical behavior of SiC/C/SiC minicomposites and modeled the deformation under a constant load in air oxidizing environment at temperatures in the range of 600–800 °C. Casas et al. [26] developed a creep oxidation model for woven SiC/C/SiC composites considering the oxidation of interface and matrix, the creep of the fibers and the degradation of the mechanical properties of the fibers with time at high temperature and predicted the strain versus time under different tensile stress levels at 1000 °C and 1100 °C. Yu et al. [27] modeled the failure process and oxidation life of SiC/C/SiC minicomposites in air oxidizing environments under a tensile load at 900 °C. However, these models could not be used to simulate the residual tensile strength of SiC/C/SiC minicomposites in stressed oxidizing environments. Therefore, the numerical modeling study for SiC/SiC composites with carbon interface was still insufficient,which would largely hinder the application of SiC/SiC components.

In this paper, a new oxidation kinetics model of SiC/C/SiC minicomposites with matrix cracks was established. The silica thickness profiles along the inner wall of matrix crack and the annular pore, the length of carbon interface consumed by oxidation were derived from the oxidation kinetics model. Then, the stress profile along the fibers including the matrix crack width was firstly derived. The assumption of linear decrease in the thickness of oxide layer along the annular pore was proposed. The residual tensile strength of SiC fibers was calculated based on the assumption. The probability of failure of fibers was obtained according to the stress profile along the fibers and tensile strength change of SiC fibers. Finally, the residual tensile strength of SiC/C/SiC minicomposites in stressed oxidizing environments was calculated combining the probability of failure of fibers with the matrix cracking

model, which agrees well with the experimental results.

Oxidation kinetics model

Filipuzzi et al. [10] proposed an oxidation kinetics model of SiC/C/SiC minicomposites in nonstress oxidizing environments, which is based upon the hypothesis that there is no matrix crack in the minicomposite and oxygen enters the interior to react with SiC fibers, carbon interface and SiC matrix from both ends of the minicomposite. In addition, the model was considered as an axisymmetrical assembly of (1) one single straight fiber (assumed to be of constant diameter $2r_{f_0}$), (2) a layer of carbon interface with a constant thickness e, (3) a shell of dense SiC matrix with a constant thickness $r_t - r_{m0}$ and (4) a "shell of porosity" taking into account the occurrence of the open porosity (Fig. 1). However, when the SiC/C/SiC minicomposites are subjected to a constant tensile stress level higher than the matrix cracking stress, a distribution of approximately parallel cracks perpendicular to the loading direction appears in the matrix, which is shown schematically in Fig. 1 [26]. Oxygen diffuses into the interior of the minicomposites mainly from the matrix cracks in stressed oxidizing environments, and the oxidation kinetics model derived by Ludovic Filipuzzi et al. [10] is not suitable to describe the diffusion process of oxygen in the matrix cracks and the change in internal morphology by oxidation. Thus, the oxidation kinetics model of SiC/C/SiC minicomposites applicable for stressed oxidizing environments is firstly proposed by incorporating the distribution of matrix cracks in the model of SiC/C/SiC minicomposites derived by Ludovic Filipuzzi et al. [10].
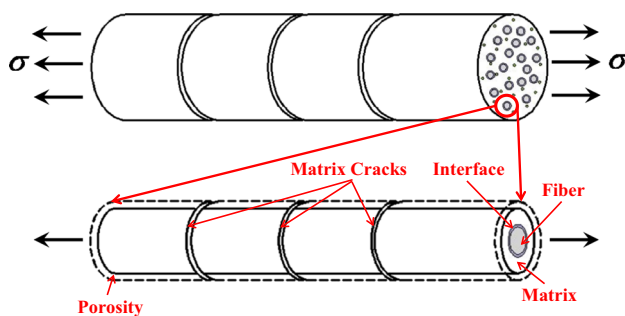

Figure 1 Model of SiC/SiC minicomposite.

Random cracking of matrix

The process of matrix crack formation and evolution are constituted by a large number of random events. In this paper, the Monte Carlo method which was described by Sun et al. [28] was used to simulate the matrix random cracking. The variations in the initial matrix crack density change as a function of tensile stress level for a SiC/C/SiC minicomposite, which is shown in Fig. 2.

As depicted from Fig. 2, the matrix crack density increases with the tensile stress level. The matrix first cracks very slow when the tensile stress level is lower than 100 MPa, and the cracking then becomes very rapid in 100–200 MPa. The matrix crack density becomes gradually saturated after the stress level is greater than 200 MPa.

Matrix crack width versus temperature and stress

According to Lamouroux's research [29], the matrix crack width of ceramic matrix composites is closely related to ambient temperature. The matrix crack width of SiC/SiC minicomposite versus applied tensile stress level was measured by Chateau et al. [30] in SEM tensile test. The experimental curve shows the matrix width increases versus the tensile stress level. The relationship between matrix crack width and temperature, tensile stress level used in this paper was derived by Sun et al. [31] in Eq. (1):

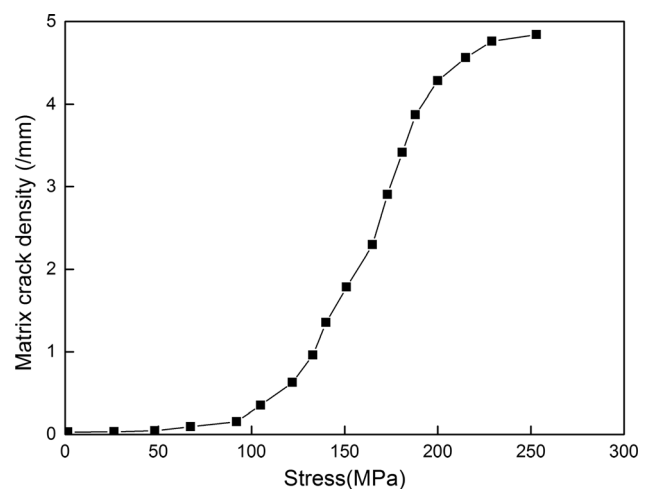$$\frac{d}{d_0} = \frac{1}{T_0}\left[\Delta T + \frac{1}{E_f V_m(\alpha_m - \alpha_f)}\sigma\right] \tag{1}$$

Figure 2 Initial matrix crack density versus stress.

where T_0 is the room temperature, d_0 denotes the matrix crack width at T_0, ΔT is the temperature difference between ambient temperature and room temperature, E_f is the Young's modulus of fiber, V_m is the volume fraction of matrix, α_m, α_f are the linear thermal expansion coefficients of matrix and fiber and σ is the tensile stress applied to the both ends of the minicomposite.

Combining the experimental data of matrix crack opening measured by Chateau et al. [30], the variations in matrix crack width as a function of temperature and tensile stress are shown in Fig. 3. It is clearly shown in Fig. 3 that the matrix crack width decreases with the increase in temperature and increases with the increase in tensile stress level before an exposure to an oxidizing atmosphere.

Oxidation of the internal porosity: model and boundary conditions

Hypotheses

The chemical reactions between the reactant and the three material components (the fibers, the interface and the matrix) are assumed to be irreversible and to take place at constant temperature and pressure. It is further assumed that (1) the concentration is constant in a given cross section of the annular pore (no radial gradients), (2) the mass transfers outside the annular pore are fast with respect to those occurring inside and (3) mass transfers by convection in the annular pore are neglected [10].
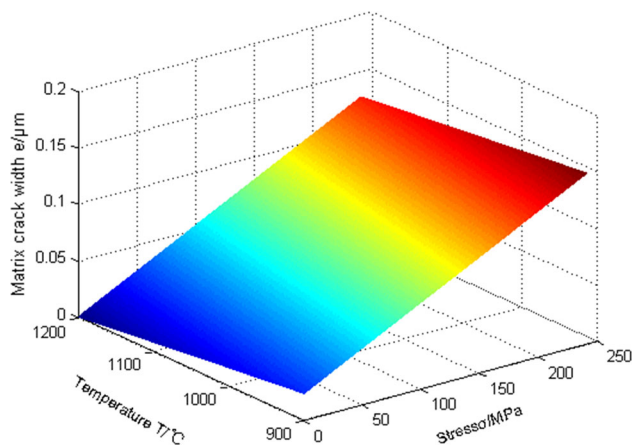

Figure 3 Initial matrix crack width versus temperature and stress.

Chemical reactions

The oxidation of carbon in an atmosphere of oxygen results in the formation of gaseous carbon oxides, according to

$$2C + O_2 = 2CO \tag{2}$$

The oxidation of silicon carbide may be depicted by the following equation:

$$SiC + \frac{3}{2}O_2 \rightarrow SiO_2 + CO \tag{3}$$

In the oxidation of the three components of the material, it is assumed that the gaseous product is CO. In the following, the calculations have been performed taking into account Eqs. (2) and (3) in order to involve the O_2/CO [10].

Oxidation kinetics equations

The diffusion of oxygen in the internal porosity of composite may be divided into two stages. In Stage I, oxygen diffuses in matrix crack and diffuses in annular pore resulting from the oxidation of carbon interface in Stage II. In the process of oxygen diffusion, the matrix crack and annular pore will become progressively filled with silica as the oxidation of walls of matrix crack and annular pore proceeds. As the oxidation time extends, the matrix crack and annular pore will be sealed by the silica layers and the process of sealing is shown in Fig. 4. The process can be divided into four cases; firstly, oxygen enters into the interior of the minicomposite and reacts with the PyC interface due to its high reaction rate at elevated temperature, which causes the removal of the PyC interface. At the same time, the oxidation of the walls of matrix cracks and annular pore occurs, which makes the SiC into SiO_2. The conversion decreases the width of matrix crack and annular pore. With the increase in time, the sealing of matrix cracks and annular pore by the silica layers occurs. The sequence of sealing depends on (1) the matrix crack width and the thickness of interface and (2) the rate of oxidation of SiC fibers and matrix.

Stage I Let us consider two cross sections of the matrix crack at z and $z + dz$, which are shown in Fig. 5. According to the law of mass conservation, the conservation equation of the number of moles of O_2
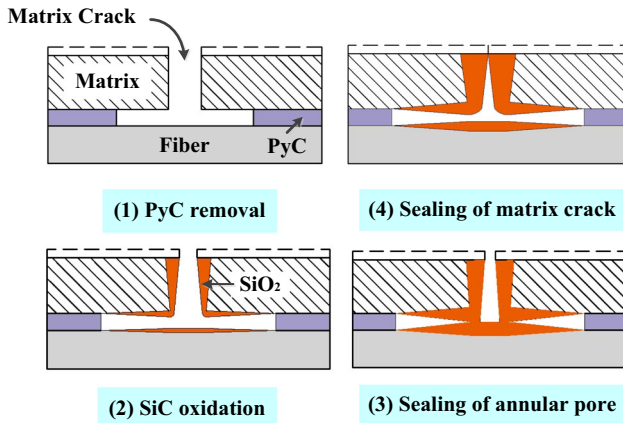
Figure 4 Geometric morphology change of matrix crack and annular pore.

diffusing across the slice of material of thickness dz during dt can be written as

$$S(z)N_{O_2}(z) - R_{O_2}(z)dz = S(z+dz)N_{O_2}(z+dz) \qquad (4)$$

where $S(z)$ is the area of the matrix crack cross section at z and $R_{O_2}(z)$ in $mol\,m^{-1}\,s^{-1}$ is the number of moles of O_2 consumed by reaction with the matrix crack walls per unit length. If dz tends toward zero, Eq. (6) can be rewritten as

$$\frac{d(SN_{O_2})}{dz} + R_{O_2} = 0 \qquad (5)$$

where N_{O_2}, the absolute molar flux of O_2, is given by

$$N_{O_2} = \frac{-D_1 C_0}{C_0 - C_{O_2}(1-\alpha)} \frac{dC_{O_2}}{dz} \qquad (6)$$

where C_0 is the total concentration, α is the ratio between the molar fluxes of O_2 and CO_2/CO, D_1 is an effective diffusion coefficient of O_2 taking into account the molecular diffusion regime and the Knudsen diffusion, which is defined as

$$D_1^{-1} = D_M^{-1} + D_{K_1}^{-1} \qquad (7)$$

where D_M is the binary diffusion coefficient (diffusion of O_2 in CO or CO in O_2) in the molecular regime, which has been calculated according to a simplified expression proposed by Fuller et al. [32]:

$$D_M = \frac{0.00143 T^{1.75}}{P\left(\frac{2}{M_{O_2}^{-1}+M_{CO}^{-1}}\right)^{1/2}[(\Sigma_v)_{O_2}^{1/3} + (\Sigma_v)_{CO}^{1/3}]^2} \qquad (8)$$

where P is the gas pressure, T is the ambient temperature, M_{O_2} and M_{CO} are the molar masses of the gaseous species O_2 and CO, $(\Sigma_v)_{O_2}$ and $(\Sigma_v)_{CO}$ are the diffusion volumes of the molecules O_2 and CO if the gaseous carbon oxide is CO, D_{K_1} is the Knudsen diffusion coefficient in matrix crack (the deriving process is in "Appendix"), which can be written as

$$D_{K_1} = \frac{2}{3}\left(\frac{8R_g T}{\pi M_{O_2}}\right)^{1/2}(2d - 2h_m) \qquad (9)$$

where R_g is the universal gas constant, d is half of the initial matrix crack width before oxidation and h_m is

Figure 5 Details of the minicomposite after an exposure to a stressed oxidizing environment.
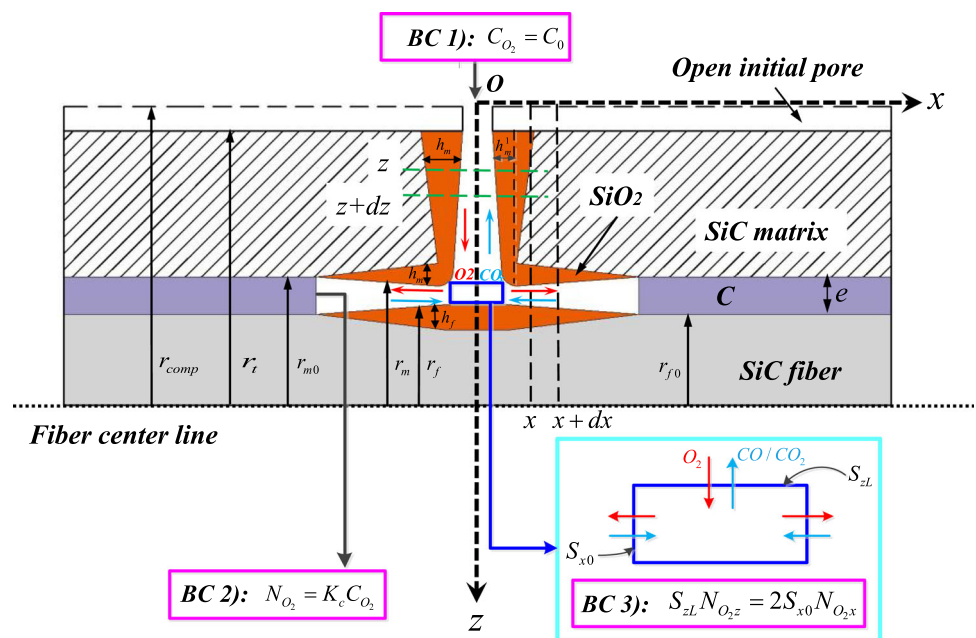
the thickness of silica scale on the matrix. The rate of growth of the silica layers on the matrix can be written as

$$\frac{dh_m(t)}{dt} = \frac{B_m^* \left(\frac{C_{O_2}}{C^*}\right)^{p_m}}{2h_m(t)} \tag{10}$$

where B_m^* and C^* are the parabolic rate constant for SiC matrix and oxygen concentration at $P = 100\,kPa$ in pure oxygen, respectively, C_{O_2} is the oxygen concentration in the internal porosity of composite and p_m is oxygen concentration exponent for SiC matrix. $S(z)$ can be written as

$$S(z) = 2\pi(r_t - z)\left(2d - 2h_m^1\right) \tag{11}$$

where h_m^1 is the thickness of expansion of oxide layer on the wall of matrix cracks, which can be expressed as

$$h_m^1 = \frac{h_m}{v_m} \tag{12}$$

where v_m is the volume expansion ratio of SiC matrix, which is given by

$$v_m = \frac{M_s}{\rho_s} \Big/ \frac{M_m}{\rho_m} \tag{13}$$

where M_s and M_m are the molar mass of silica and SiC matrix, respectively, ρ_s and ρ_m are the densities of silica and SiC matrix, respectively.

R_{O_2} denotes the number of moles of A, which is consumed by reaction with the matrix crack wall at t during dt and per unit length, which can be expressed as

$$R_{O_2} = \frac{2g_m(r_t - z)\rho_s B_m^* \left(\frac{C_{O_2}}{C^*}\right)^{p_m}}{M_s h_m} \tag{14}$$

where g_m is the number of moles of O_2 necessary to form 1 mol of silica during oxidation of SiC matrix.

Combining Eqs. (7), (8), (9) and (14), the differential equation at each time t is

$$\frac{d}{dz}\left[2(r_t - z)\left(2d - 2h_m^1(z, t)\right)\frac{-D_1 C_0}{C_0 - C_{O_2}(1 - \alpha)}\frac{dC_{O_2}}{dz}\right]$$
$$+ \frac{2g_m(r_t - z)\rho_s B_m^* \left(\frac{C_{O_2}}{C^*}\right)^{p_m}}{M_s h_m}$$
$$= 0 \tag{15}$$

All of the second-order terms, i.e., dh_m/dz, dD_1/dz and $d\alpha/dz$, are taken into account in the resolution procedure.

Stage II Similar to Stage I, two cross sections of the matrix crack at x and $x + dx$ were considered, which are shown in Fig. 5. The area of the annular pore cross section can be written as

$$S(x) = \pi\left(r_m^2 - r_f^2\right) \tag{16}$$

The differential equation at time t is

$$\frac{d}{dx}\left[\left(r_m^2 - r_f^2\right)\frac{-D_2 C_0}{C_0 - C_{O_2}(1 - \alpha)}\frac{dC_{O_2}}{dx}\right]$$
$$+ \frac{g_m r_m \rho_s B_m^* \left(\frac{C_{O_2}}{C^*}\right)^{p_m}}{2M_s h_m} + \frac{g_f r_f \rho_s B_f^* \left(\frac{C_{O_2}}{C^*}\right)^{p_f}}{2M_s h_f}$$
$$= 0 \tag{17}$$

where D_2 is an effective diffusion coefficient of O_2 in annular pore, which can be written as

$$D_2^{-1} = D_M^{-1} + D_{K_2}^{-1} \tag{18}$$

where D_{K_2} is the Knudsen diffusion coefficient in annular pore, which is given by [10]

$$D_{K_2} = \frac{2}{3}\left(\frac{8R_g T}{\pi M_{O_2}}\right)^{1/2}(r_m - r_f) \tag{19}$$

g_f is the number of moles of O_2 necessary to form 1 mol of silica during oxidation of SiC fiber, B_f^* and p_f are the parabolic rate constant and oxygen concentration exponent for SiC Matrix, respectively, and h_f is the thickness of silica scale on the SiC fiber. The rate of growth of the silica layers on the fiber can be written as

$$\frac{d[h_f(t)]}{dt} = \frac{B_f^* \left(\frac{C_{O_2}}{C^*}\right)^{p_f}}{2h_f(t)} \tag{20}$$

Boundary conditions

The boundary conditions are given by

1. At the top of matrix crack ($z = 0$), with
   $$C_{O_2} = C_0 \tag{21}$$

2. At the end of interfacial oxidation, with
   $$\frac{-D_2 C_0}{C_0 - C_{O_2}(1 - \alpha)}\frac{dC_{O_2}}{dz} = K_c C_{O_2} \tag{22}$$

The oxidation rate of the carbon interface at t is given by

$$\frac{d(l_r)}{dt} = -bD_2(l_r)\frac{M_c}{\rho_c}\left(\frac{dC_{O_2}}{dz}\right)_{l_r}\frac{C_0}{C_0 + (1-\alpha)C_{O_2}(l_r)},$$

$$(23)$$

where b is the number of moles of carbon oxidized per mole of O_2 and M_c and ρ_c are the molar mass and density of carbon, respectively.

3. At the bottom of matrix crack ($z = r_t - r_{m0}, x = 0$), it is assumed that there is no consumption of oxygen at this region where the number of moles of oxygen entering the bottom of matrix crack is equal to that entering the two entrances of the annular pore (Fig. 5), with

$$S_{zL}N_{O_2z} = 2S_{x0}N_{O_2x} \qquad (24)$$

where S_{zL} and S_{x0} are the area of the bottom of matrix crack and the entrance of the annular pore, respectively. Combining Eqs. (9) and (24), Eq. (24) can be rewritten as

$$2\pi(r_t - z)\left(2d - 2h_m^1(t)\right)\frac{-D_1C_0}{C_0 - C_{O_2}(1-\alpha)}\frac{dC_{O_2}}{dz}$$
$$= \pi\left(r_m^2 - r_f^2\right)\frac{-D_2C_0}{C_0 - C_{O_2}(1-\alpha)}\frac{dC_{O_2}}{dx}$$

$$(25)$$

Numerical solution

The classical Runge–Kutta algorithm was used to solve Eqs. (20) to (25), (13), (15), (17) based on the known boundary conditions. The second-order differential Eqs. (15) and (17) were converted into first-order differential equations by changing $\frac{dC_{O_2}}{dx}, \frac{dC_{O_2}}{dz}$ to p, q and making $p' = \frac{d^2C_{O_2}}{dx^2}, q' = \frac{d^2C_{O_2}}{dz^2}$. The length of matrix crack and annular pore was divided evenly into 100 grids. The time step was set to 1 s.

The results of the calculations were expressed as (1) the silica thickness profiles, along the matrix crack and annular pore, for each time t in stressed oxidizing environment and (2) the length of carbon consumed by oxidation at each time t.

The oxidation of the open initial pore has a great effect on the mass variation of SiC matrix, but it has almost no effect on the oxidation of SiC fibers and C interface [10]. Thus, the oxidation of the open initial pore was not taken into account in the present model.

Model of residual strength of SiC/C/SiC minicomposites

Consider an ideal unidirectional SiC/SiC composite, and the fibers are assumed to be coated with a carbon layer, which is shown in Fig. 1. The composite is subjected to a constant tensile stress, σ, at high temperature. When the applied stress is higher than the matrix cracking stress, a distribution of approximately parallel cracks perpendicular to the loading direction appears in the matrix [26]. The matrix crack density and width versus temperature and tensile stress, which are shown in Figs. 2 and 3, were adopted to describe the fiber stress distribution. According to Curtin's research [33], the average distribution of matrix cracks in the model has a little effect on the accuracy of predicted tensile strength. Thus, the matrix cracks are assumed to be equally spaced at a distance L_c and a characteristic element including a single fiber and surrounding matrix between adjacent cracks is selected to analyze the fiber stress distribution, which is shown in Fig. 6. The fiber stress distribution under stressed oxidizing environment has been studied in the past two decades [9, 26, 34, 35]; however, these studies did not take the fiber stress distribution corresponding to the matrix crack width. In this paper, the fiber stress distribution corresponding to the matrix crack width was firstly derived. Lara-Curzio [36] studied the relationship of the residual strength of SiC fibers under oxidizing environment with the thickness of the oxide layer. The distribution of the thickness of the oxide layer is not the same. In this paper, the assumption of the linear decrease in the thickness of the oxide layer along the annular pore was proposed. Based on this assumption and the equation derived by Lara-Curzio [36], the residual strength of SiC fibers under oxidizing environment was calculated. The fiber stress distribution and residual strength of SiC fibers were brought into the equation derived by Casas et al. [26] to calculate the probability of failure of the fibers. In this process, the section integration of the probability of failure of the fibers considering the fiber stress distribution in the matrix crack was derived in this paper. Combining the probability of failure of the fibers with the matrix cracking model proposed by Curtin [37], the residual strength of SiC/SiC minicomposites in stressed oxidizing environment was calculated.

Figure 6 Fiber stress distribution between two matrix cracks.
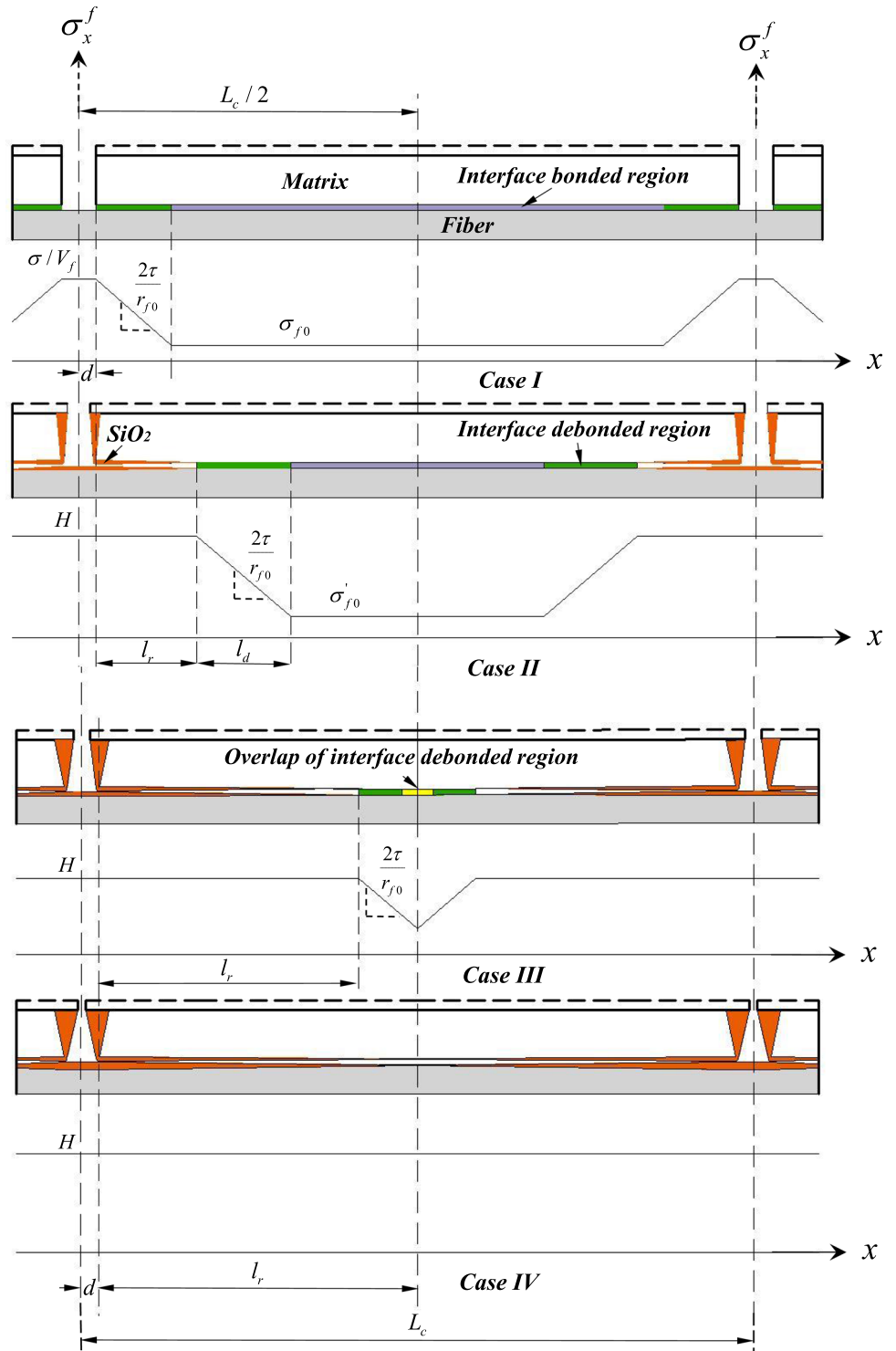
Fiber stress distribution

There are four different forms in the fiber stress distribution during the high-temperature stress-oxidation process of composite, which is shown in Fig. 6.

After matrix cracking, the axial stress in the fiber will increase in the crack plane to support the entire stress of the composite. Away from the matrix crack plane, the fiber stress decreases and satisfies the following equation [26]

$$\frac{d\sigma_x^f}{dx} = -\frac{2\tau}{r_{f_0}} x \tag{26}$$

where r_{f_0} is the fiber radius, τ is the interfacial shear stress and x represents the axial distance to the matrix crack plane.

Case I

When the composite is subjected to a tensile load before an exposure to an oxidizing atmosphere, the stress distribution along the fiber, which is shown in Case I of Fig. 6, can be expressed as

$$\sigma_x^f(x) = \begin{cases} \dfrac{\sigma}{V_f}, & x \in (0,d) \\ \dfrac{\sigma}{V_f} - \dfrac{2\tau}{r_{f_0}}x, & x \in (d, d+l_d) \\ \sigma_{f_0}, & x \in (d+l_d, L_c/2) \end{cases} \tag{27}$$

where l_d is the length of interface debonded region and σ_{f_0} denotes the stress in interface bonded region, which can be expressed as

$$\sigma_{f_0} = E_f \frac{\sigma}{E_c} \tag{28}$$

where E_f and E_c are initial elastic modulus of fibers and composite, respectively.

Case II

When the composite is exposed to the stressed oxidizing environment for a time, the carbon interface will be consumed by oxidation, where the stress distribution along the fiber will be influenced (Case II of Fig. 6). Due to the existence of the tensile stress, the interface debonded region still exists. It is assumed that the interface debonded regions between two cracks are not overlapped, and the stress distribution along the fiber can be described by Eq. (31):

$$\sigma_x^f(x)$$
$$= \begin{cases} H(t), & x \in (0, d+l_r) \\ H(t)[U(x)] - \dfrac{2\tau}{r_{f0}}(x \\ \quad - l_r(t) - d)[U(x - l_r(t) - d)], & x \in (d+l_r, d+l_r+l_d) \\ \sigma'_{f_0}, & x \in (d+l_r+l_d, L_c/2) \end{cases} \tag{29}$$

where $H(t)$ is the maximum axial stress in the fiber in the matrix crack plane and $U(x - x_0)$ is unit step function, which is given by

$$U(x - x_0) = \begin{cases} 1 & x > x_0 \\ 0 & x < x_0 \end{cases} \tag{30}$$

Assuming global load sharing conditions, a simple force balance at the matrix crack plane provides the relationship between the stress applied to the composite, σ, and the maximum axial stress in the fiber, $H(t)$,

$$\sigma = V_f \left[H(t)(1 - \Phi_L) + \frac{2\tau}{r_{f_0}} \lambda \Phi_L \right] \tag{31}$$

where λ is the average fiber pullout and Φ_L is the probability of failure of the fibers, which will be discussed in "Probability of failure of the fibers" section.

The equilibrium stress in interface bonded region, σ'_{f_0}, can be expressed as

$$\sigma'_{f_0} = \frac{E_f \sigma}{E_f V_f (1 - \Phi_L) + E_m V_m} \tag{32}$$

At $x = d + l_r + l_d$, there is a simple force balance between the stress in interface debonded region, $\sigma_x^f(x)$, and the stress in interface bonded region, σ'_{f_0}.

$$\sigma_x^f(d + l_r + l_d) = \sigma'_{f_0} \tag{33}$$

Combining Eqs. (29), (32) and (33), the length of interface debonded region, l_d, can be calculated.

Case III

When the oxidation time increases, the carbon interface length consumed by oxidation, l_r, increases gradually and the overlap of interface debonded regions between two cracks may occur (Case III of Fig. 6). The stress distribution along the fiber can be written as

$$\sigma_x^f(x) = \begin{cases} H(t), & x \in (0, d+l_r) \\ H(t)[U(x)] - \dfrac{2\tau}{r_{f_0}}(x - l_r(t) \\ \quad - d)[U(x - l_r(t) - d)], & x \in (d+l_r, L_c/2) \end{cases} \tag{34}$$

Case IV

Finally, if the carbon interface in the characteristic element is consumed completely, the stress in the fiber, $\sigma_f(x)$, remains unchanged as the maximum

axial stress in the fiber in the matrix crack plane, $H(t)$, which is shown in Case IV of Fig. 6.

Residual strength of fibers

While the carbon interface is consumed by oxidation, the SiC fibers are oxidized by oxygen in stressed oxidizing environments, and the oxidized product, silica, will adhere to the surface of the fibers to form oxide layers [38], which is shown in Fig. 7a. Due to the existence of oxide layers, the fiber strength decreases. Gogotsi et al. [18] showed that the strength of SiC fibers is inversely proportional to the square root of the oxide layer thickness on the surface of the fibers. From the standpoint of fracture mechanics, the relationship between fiber toughness, K_{IC}, and fiber strength, σ_f, is given by [36]

$$K_{IC} = Y\sigma_f\sqrt{\delta} \tag{35}$$

where Y is a shape factor and δ is the defect size, which is the thickness of SiC fibers consumed by oxidation and is proportional to the thickness of the oxide layers. It is assumed that the strength of the fibers, σ_f, remains constant until the oxide layer becomes larger than the critical defect size, a. The critical defect size can be written as [36]

$$a = \left(\frac{K_{IC}}{Y\bar{\sigma}_f}\right)^2 \tag{36}$$

where $\bar{\sigma}_f$ is the initial tensile strength of the fiber. It is assumed that the fiber toughness remains constant

Figure 7 Residual strength of Nicalon fibers versus defect size.

and the shape factor does not vary significantly with the defect size [18, 26, 34]. Then, the fiber strength can be rewritten as

$$\sigma_f = \begin{cases} \bar{\sigma}_f & \delta \leq a \\ \dfrac{\bar{\sigma}_f}{\sqrt{\delta}}\sqrt{a} & \delta > a \end{cases} \tag{37}$$

The residual strength of Nicalon fibers versus defect size is depicted in Fig. 7b.

In the present model, the oxide layer on the surface of fiber along fiber can be divided into two parts: (1) the oxide layer in the matrix crack and (2) the oxide layer in the interface consumption region.

Due to the difference in oxygen concentration along the annular pore, the thickness of oxide layer along the fiber is different. The thickness of oxide layer in the matrix crack is the largest, while that in the interface consumption region decreases along the annular pore. It is assumed that the thickness of oxide layer at the carbon interface is equal to zero, which is shown in Fig. 8a. Based on the calculated results of the oxide layer in the matrix crack, hf_{int}, the defect size in the matrix crack, $\delta(d)$, can be expressed as

$$\delta_d(t) = \frac{hf_{int}(t)}{v_f} \tag{38}$$

where v_f is the volume expansion ratio of SiC fiber, which is given by

$$v_f = \frac{x_1 M_s}{\rho_s} \Bigg/ \frac{M_{Si_{x_1}C_{y_1}O_{z_1}}}{\rho_{Si_{x_1}C_{y_1}O_{z_1}}} \tag{39}$$

where $Si_{x_1}C_{y_1}O_{z_1}$ is the chemical formula for SiC fiber, $M_{Si_{x_1}C_{y_1}O_{z_1}}$ is the molar mass of SiC fiber and $\rho_{Si_{x_1}C_{y_1}O_{z_1}}$ is the density of SiC fiber.

After a short exposure to stressed oxidizing atmosphere for the composite, the thickness of oxide layer on the fiber surface in the matrix crack, $\delta(d)$, is less than the critical defect size, a. Thus, the fiber strength in the oxidation section of fiber can be expressed as

$$\sigma_f(x, t) = \bar{\sigma}_f \quad x \in (0, d + l_r) \tag{40}$$

When the thickness of oxide layer on the fiber surface in the matrix crack is greater than the critical defect size, the loss of fiber strength occurs. It is assumed that the defect size decreases linearly along the annular pore, which is given by
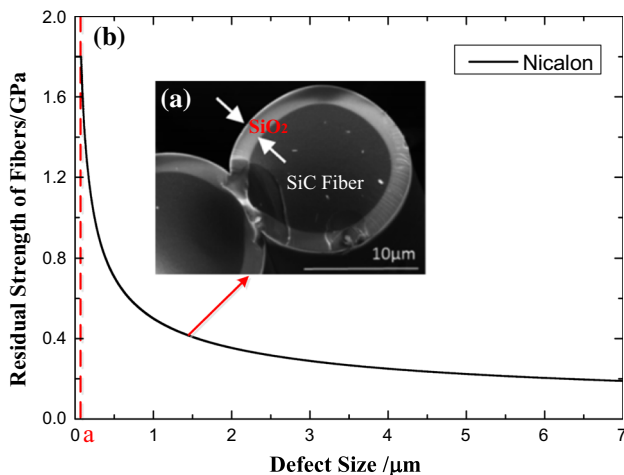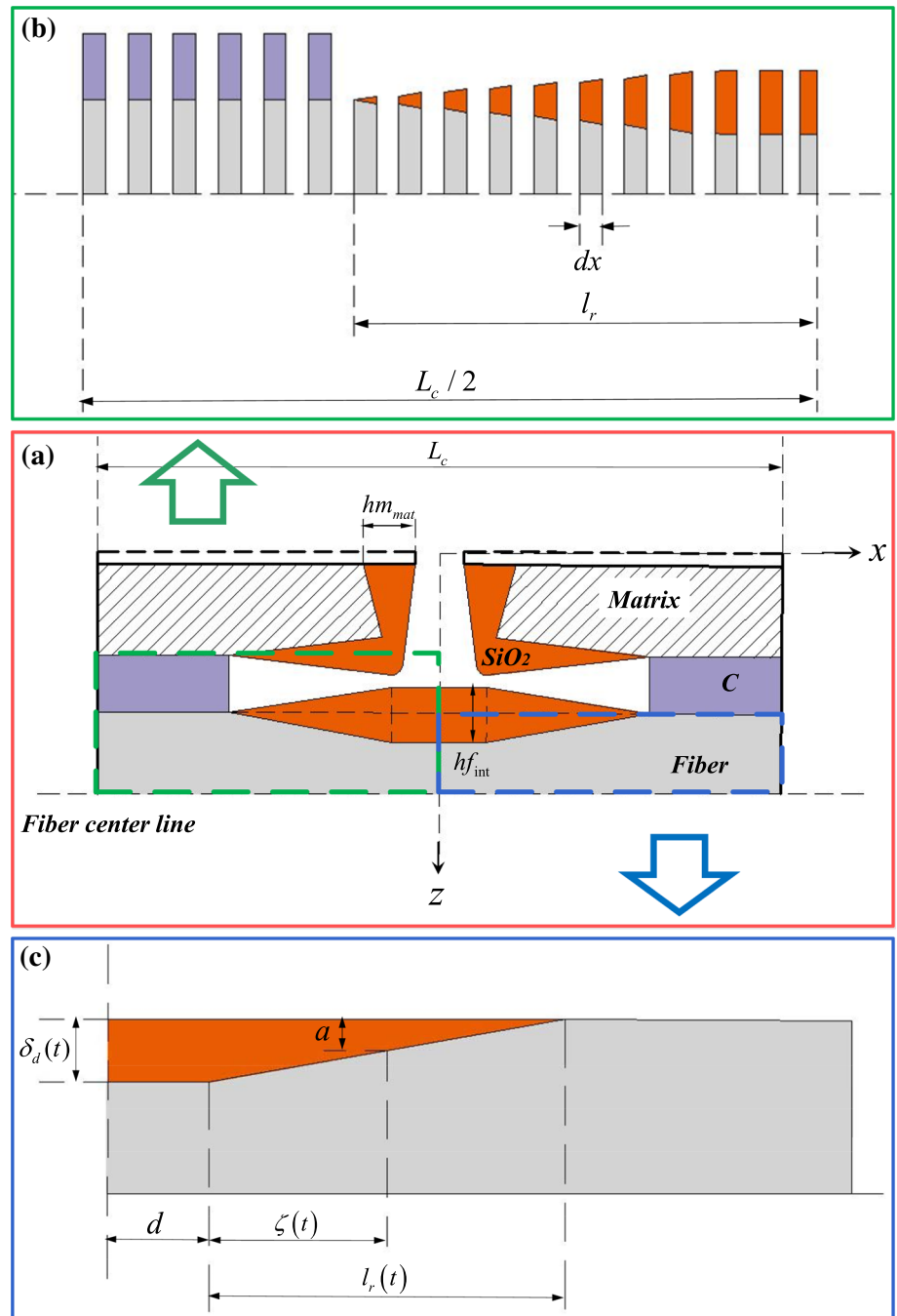
Figure 8 Schematic of details of oxidation of interface and fibers.

Let the distance from the critical defect size to the center line of matrix crack be $\zeta(t)$, which is shown in Fig. 8c, then the fiber strength can be expressed as

$$\delta(x,t) = \begin{cases} \delta_{\mathrm{d}}(t) & x \in (0,d) \\ \dfrac{l_{\mathrm{r}}(t)}{l_{\mathrm{r}}(t)+d-x}\delta_{\mathrm{d}}(t) & x \in (d,d+l_{\mathrm{r}}) \end{cases} \quad (41)$$

$$\sigma_{\mathrm{f}}(x,t) = \begin{cases} \dfrac{\bar{\sigma}_{\mathrm{f}}}{\sqrt{\delta_{\mathrm{d}}(t)}}\sqrt{a} = \sigma_{\mathrm{d}}(t) & x \in (0,d) \\ \sqrt{\dfrac{l_{\mathrm{r}}(t)}{l_{\mathrm{r}}(t)+d-z}}\sigma_{\mathrm{d}}(t) & x \in (d,d+\zeta) \\ \bar{\sigma}_{\mathrm{f}} & x \in (d+\zeta,d+l_{\mathrm{r}}) \end{cases} \quad (42)$$

Probability of failure of the fibers

With the increase in oxidation time, the fibers will break in the stressed oxidizing environment. A two-parameter Weibull distribution has been used to describe the strength of the fibers. Then, the probability of failure of the fibers is given by [26]:

$$\Phi_L = 1 - \exp\left\{ - \int_{L_g} \frac{1}{l_0} \left(\frac{\sigma_x^f(x)}{\sigma_0(x,t)} \right)^m dx \right\} \quad (43)$$

where L_g is the length of integral segment, m is the Weibull modulus, σ_0 is the characteristic strength for a fiber with the reference length l_0, which will change versus oxidation time and location, and the degradation rule of characteristic strength of a fiber is shown in "Residual strength of fibers" section.

The unit cell, which is shown in Fig. 8a, is discretized into differential elements of length dx as illustrated in Fig. 8b. Combining the fiber stress distribution ("Fiber stress distribution" section) and Eq. (43), the probability of failure of the fibers can be rewritten as

$$\Phi_L = 1 - \exp\left\{ - \frac{2L}{L_c l_0} (I_1 + I_2 + I_3 + I_4 + I_5) \right\} \quad (44)$$

where I_1, I_2, I_3, I_4, I_5 can be expressed, respectively, as

$$
\begin{cases}
I_1 = \int_0^d \left(\dfrac{H}{\sigma_0(x,t)} \right)^m dx \\[2mm]
\quad = d \left(\dfrac{H}{\sigma_{d0}(t)} \right)^m \\[3mm]
I_2 = \int_d^{d+\zeta} \left(\dfrac{H}{\sigma_0(x,t)} \right)^m dx \\[2mm]
\quad = \dfrac{2 \left[l_r(t)^{(m/2+1)} - (l_r(t) - \zeta(t))^{(m/2+1)} \right]}{(m+2) l_r(t)^{(m/2)}} \left(\dfrac{H}{\sigma_{d0}(t)} \right)^m \\[3mm]
I_3 = \int_{d+\zeta}^{d+l_r} \left(\dfrac{H}{\sigma_0(x,t)} \right)^m dx \\[2mm]
\quad = (l_r(t) - \zeta(t)) \left(\dfrac{H}{\bar{\sigma}_0} \right)^m \\[3mm]
I_4 = \int_{d+l_r}^{d+l_r+l_d} \left(\dfrac{\sigma_x^f}{\sigma_0(x,t)} \right)^m dx \\[2mm]
\quad = \dfrac{r_{f_0}}{2\tau(m+1)\bar{\sigma}_0^m} \left(H^{m+1} - (H - 2\tau l_d / r_{f_0})^{m+1} \right) \\[3mm]
I_5 = \int_{d+l_r+l_d}^{L_c/2} \left(\dfrac{\sigma_x^f}{\sigma_0(x,t)} \right)^m dx \\[2mm]
\quad = (L_c/2 - d - l_r(t) - l_d) \left(\dfrac{\sigma_{f_0}}{\bar{\sigma}_0} \right)^m
\end{cases}
$$

$$(45)$$

where $\bar{\sigma}_0$ is the initial characteristic strength of fibers before an exposure to oxidizing environment. After Eqs. (31), (44), (45) are combined, the probability of failure of the fibers can be calculated.

Matrix cracking model

SiC/SiC composites become brittle due to oxidation of the constituents in stressed oxidizing environments, which leads to the short fiber pullout and the fact that the breakage of fibers occurs in oxidized part of fibers [39]. The matrix cracking model, including the single matrix cracking model and multimatrix cracking model, was used to calculate the residual tensile strength of SiC/C/SiC minicomposites [40]. It is assumed that the multimatrix cracking model can be used to calculate the residual tensile strength of the composite of short carbon interface length consumed by oxidation due to an exposure to an oxidizing atmosphere for a short time. When the unoxidized interface is insufficient to support the appearance of new matrix crack, which can be expressed as

$$(L_c/2 - l_r - d) < l_e, \quad (46)$$

the single matrix cracking model was used to model the residual tensile strength of the composite, where l_e is the saturated average matrix crack spacing.

Multimatrix cracking model

Multimatrix cracking means that multiple cracks occur in the matrix during the process of actual tensile test. When the tensile stress level reaches a critical value, the matrix cracks will be saturated. The breakage of fibers will occur with the increase in tensile stress. According to Curtin's study [37], the breakage of fibers at the matrix cracks and in the range of interfacial debonding length is only needed to be considered for calculation of the probability of failure of the fibers. The occurrence of matrix cracks can be divided into two stages: (1) the matrix cracks occur in the oxidizing environment with a constant tensile load and (2) the matrix cracks occur in the test of residual tensile strength at room temperature. Only the fibers at the matrix cracks, which occur in the first stage, can be oxidized. Thus, the average probability of failure of the fibers at the matrix cracks is given by

$$q = \phi(\Phi_o + \Phi_m) + (1 - \phi)\Phi_m \qquad (47)$$

where ϕ is the ratio of the number of matrix cracks in the first stage to the number of matrix cracks in all the two stages, which is related to the external tensile stress level σ, Φ_o is the probability of failure of oxidized part of the fibers, which is given by

$$\Phi_o = 1 - \exp\left\{-\frac{1}{l_0}\left[d\left(\frac{S}{\sigma_{d0}(t)}\right)^m + \frac{2\left[l_r^{(m/2+1)} - (l_r - \zeta)^{(m/2+1)}\right]}{(m+2)l_r^{(m/2)}}\right.\right.$$
$$\left.\left.\times\left(\frac{S}{\sigma_d(t)}\right)^m + (l_r - \zeta)\left(\frac{S}{\bar{\sigma}_0}\right)^m\right]\right\} \qquad (48)$$

where S is the maximum axial stress in the fiber for the test of residual strength of the composite.

Φ_m is the probability of failure of fibers in the range of interface debonded length, which is derived by Curtin et al. as [33]

$$\Phi_m = 1 - \exp\left\{-\frac{r_{f_0}S^{m+1}}{\tau l_0(m+1)\bar{\sigma}_0^m}\left[1 - \left(1 - \frac{l_e}{l_s}\right)^m\right]\right\} \qquad (49)$$

where l_s is the critical length of interface slip.

When the matrix cracks are saturated, the overlap of interface debonded regions near the cracks will occur and the number of matrix cracks in the interface debonded regions of any crack can be expressed as $1 + 2l_s/l_e$. If the breakage of fibers randomly occurs in the matrix cracks, the average fiber pullout is long and the stress needed for fiber pullout is large. The axial stress in the fiber can be expressed as

$$F = \frac{\sigma}{V_f(1 - \Phi_L)} = \left(1 - q\left(1 + \frac{2l_s}{l_e}\right)\right)S + q\frac{2l_s}{l_e}\frac{S}{2} \qquad (50)$$

By taking a derivative of the maximum axial stress in the fiber, S, and making the derivative be zero, $dF/dS = 0$, the maximum value of S can be obtained. The residual strength of the composite, σ_{uts}, can be obtained by bringing the maximum value of S into Eq. (50).

Single matrix cracking model

The single matrix cracking refers to the situation that the composite only breaks at the matrix cracks under the external load and the fiber pullout is equal to zero. When the oxidation time is long, the length of carbon interface consumed by oxidation is long and the oxidation of fibers is serious, which makes the

fracture mode of the composite transform into brittle fracture. The average probability of failure of fibers under this fracture mode is given by

$$p = \Phi_o \qquad (51)$$

The axial stress in the fiber can be expressed as

$$F = \frac{\sigma}{V_f(1 - \Phi_L)} = (1 - p)S \qquad (52)$$

The residual strength of the composite can be calculated by adopting the same way as illustrated in "Multimatrix cracking model" section.

Results and discussion

In this paper, the oxidation kinetics equations were firstly established.

By solving these equations, the length of carbon interface consumed by oxidation, the silica thickness on fiber at interface entrance and the silica thickness at the top of matrix crack were calculated. Then, the fiber stress distribution, the fiber residual strength and the probability of failure of fibers were calculated. The residual strength of SiC/SiC minicomposites was obtained with the matrix cracking model. The simulation procedure of residual strength of the composite is shown in Fig. 9.

During this procedure, it is assumed that the oxidation of the SiC fibers and C interface is stopped when the annular pore sealing or matrix crack sealing occurs. The variations in the residual tensile strength after the sealing of annular pore or matrix crack are not taken into account in the present model.

Characteristic parameters of the oxidation kinetics model

In the present model, three characteristic parameters were selected to describe the change in geometry of the composite such as the length of carbon interface consumed by oxidation l_r, the silica thickness on fiber at interface entrance hf_{int} and the silica thickness at the top of matrix crack hm_{mat}, which are shown in Fig. 8.

The silica thickness at the top of matrix crack was used to describe the sealing state of matrix cracks, and the silica thickness on fiber at interface entrance was used to describe the sealing state of interface. Using the numerical values listed in Table 1, the
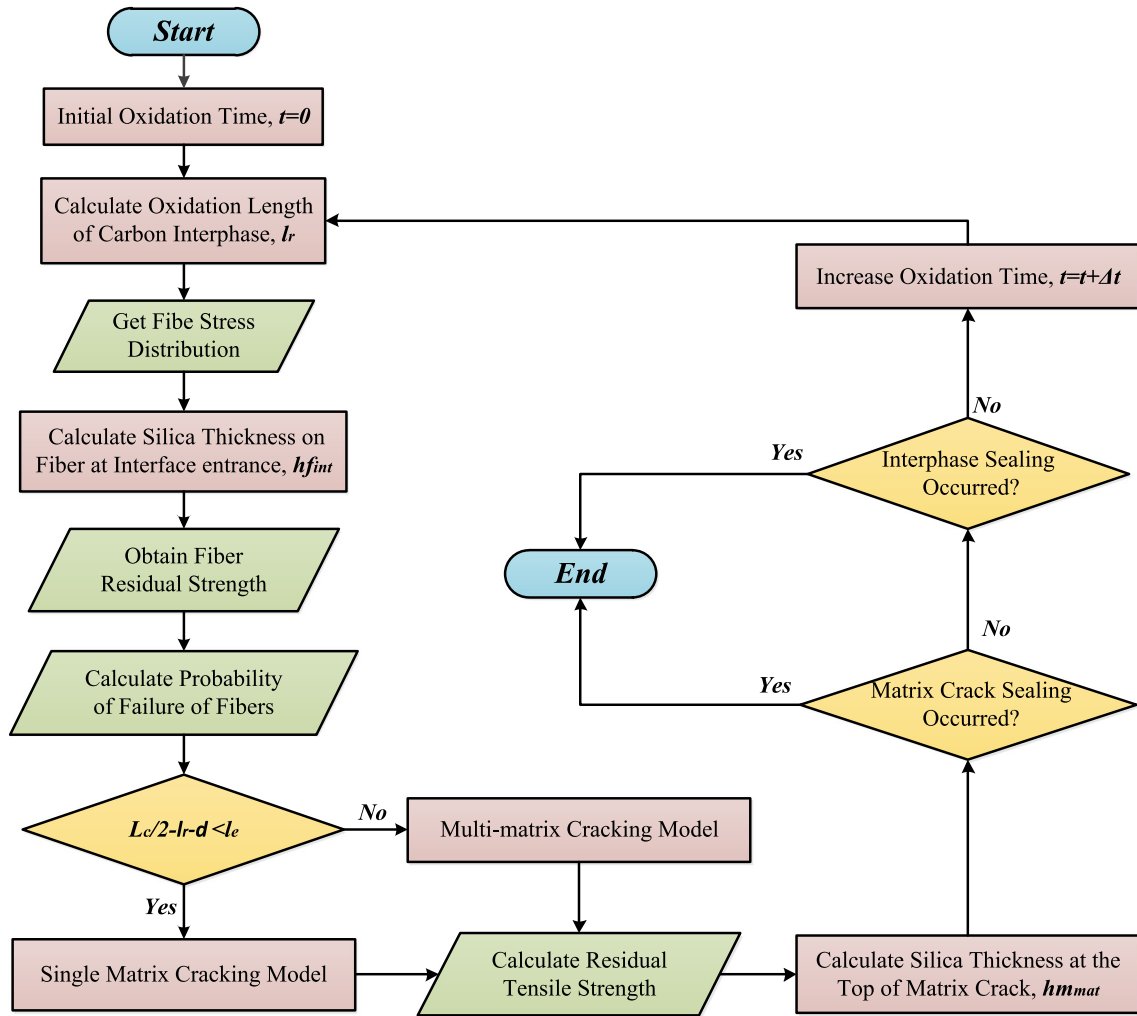
Figure 9 Simulation procedure of residual strength of the composite.

changes in characteristic parameters as a function of time at four different temperatures (900 °C, 1000 °C, 1100 °C and 1200 °C) under a constant tensile stress level (80 MPa, 200 MPa) are shown in Figs. 10, 11 and 12.

As shown in Fig. 10, the silica thickness at the top of matrix crack, hm_{mat}, shows a parabolic increase with the increase in time. It clearly appears from Fig. 10 that the initial slope increases with the increase in temperature, which indicates that the growth rate of oxide layer becomes higher when the temperature increases. This is due to the increase in oxidation rate between SiC and O_2 with temperature increasing.

Conversely, as the oxidation proceeds further, the reverse phenomenon is observed. As a matter of fact, when the temperature is raised, the value of sealing time and that of the silica thickness at the top of

matrix crack both decrease. At low temperatures, the silica on the matrix crack grows slowly but over a wide matrix crack, whereas at high temperatures the oxidation of SiC matrix is rapid but limited to a narrow matrix crack.

The sealing time under the tensile stress level of 80 MPa is much shorter than that under the tensile stress level of 200 MPa at the same temperature, which is also due to the different matrix crack width. For $\sigma = 80$ MPa, the matrix cracks are narrower and oxide layers can seal them in shorter time to prevent the further diffusion of oxygen in the matrix cracks. Furthermore, it is clear from the figure that the trend of the increase in thickness of oxide layer under different stress levels is almost the same, which indicates the stress level has low effect on the oxidation behavior of SiC matrix and just affects the sealing
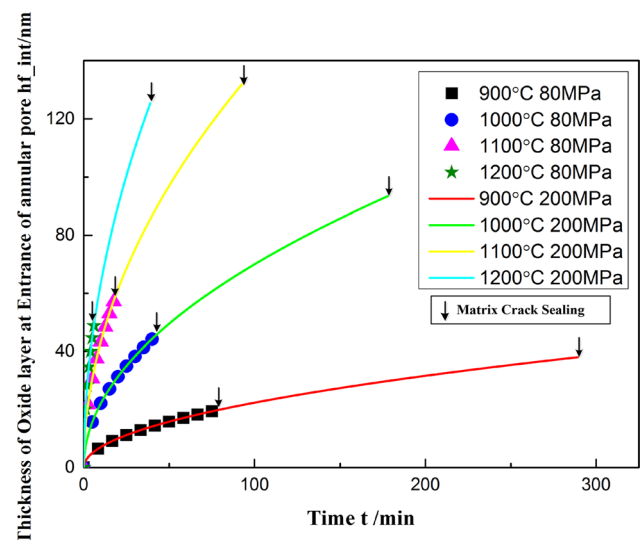
Table 1 Material parameters of the model

Parameter	Symbol	Value	Ref.
Fiber radius	r_{f_0}	7 μm	[10]
Thickness of carbon interface	e	0.1 μm	[10]
Energy of activation	E_c	104.433 kJ mol^{-1}	[41]
Fiber volume fraction	V_f	42%	[10]
Matrix volume fraction	V_m	58%	
Gas constant	R	8.3145 J (mol*K)$^{-1}$	[10]
The initial crack width under tensile stress level of 200 Mpa	d_0	0.2 μm	[30]
Density of matrix	ρ_m	3.2×10^3 kg m^{-3}	[10]
Density of fiber	ρ_f	2.55×10^3 kg m^{-3}	[10]
Coefficient of thermal expansion for matrix	α_m	4.6×10^{-6} °C^{-1}	[42]
Coefficient of thermal expansion for fiber	α_f	3.1–3.5×10^{-6} °C^{-1}	[42]
Weibull modulus of carbon fibers	m	3.5	[35]
Characteristic strength for a fiber	σ_0	1.8 GPa	[35]
Original shear stress of interface	τ	4 MPa	[35]
Reference length	l_0	25 mm	[35]
Young's modulus of fiber	E_f	200 GPa	[35]
Young's modulus of matrix	E_m	400 GPa	[26]
Ratio of fiber toughness to a shape factor	K_{IC}/Y	0.5 MPa m$^{-0.5}$	[34]
Fiber pullout	λ	0.37–0.75 mm	[39]
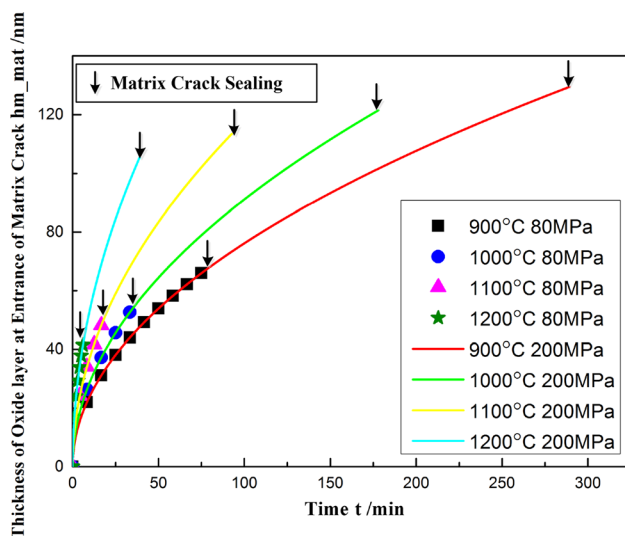
Figure 10 Variations in the calculated silica thickness at the top of matrix crack.

Figure 11 Variations in the thickness of oxide layers on the surface of SiC fibers at the entrance of the annular pore.

time of the matrix cracks by controlling the matrix crack width.

The variations in the thickness of oxide layers on the surface of SiC fibers at the entrance of annular pore as a function of time under various stress levels at different temperatures are shown in Fig. 11. As expected, the thickness of oxide layers on the surface

of SiC fibers at the entrance of annular pore, hf_{int}, shows a parabolic increase with increase in time, which is similar to the oxidation of SiC matrix. The sealing time of the annular pore and the matrix crack is almost the same under the same tensile stress level at the same temperature by comparing Figs. 10 and 11, which indicates the matrix cracks are firstly sealed
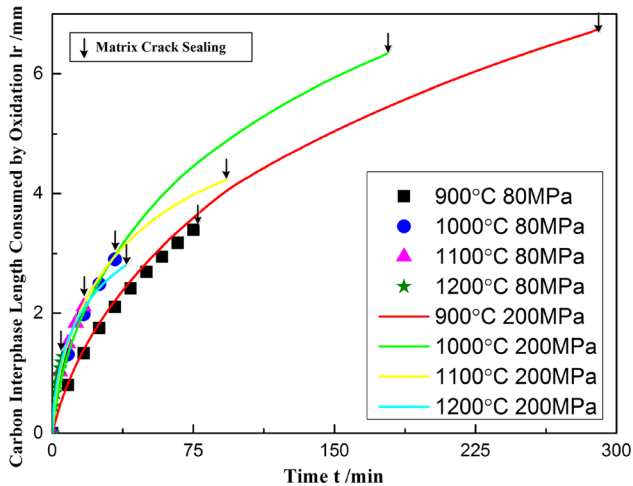
Figure 12 Variations in the length of carbon interface consumed by oxidation.

under the tensile stress level of 80–200 MPa at the temperature range of 900–1200 °C. As the matrix cracks are sealed firstly, the external oxygen cannot enter the interior of the composite and the fibers cannot be further oxidized, which indicates that the internal oxidation of the composites is controlled by the sealing of matrix cracks.

The variations in the length of carbon interface consumed by oxidation as a function of time under various stress levels at different temperatures, calculated from the model, are shown in Fig. 12.

As expected, the kinetics of growth of l_r decrease rapidly with increasing oxidation time, which is due to (1) the reaction of the pore wall (SiC fibers and matrix) with oxygen and (2) the geometry of the annular pore changes with time, which leads to decrease in the amount of oxygen entering to the annular pore. Furthermore, the reaction rate of carbon interface is expected to increase as the temperature is increased.

The sealing time and the length of carbon interface consumed by oxidation under different tensile stress levels at 900 °C are shown in Table 2. As already mentioned above, both the sealing time of matrix cracks and the length of carbon consumed by oxidation increase with the increase in the tensile stress level, which indicates that the tensile stress level cannot change the oxidation behavior of the composite, and just change the amount of oxygen entering the annular pore by changing the matrix crack width. It is assumed that the oxidation of carbon interface stops when the matrix cracks are sealed.

Residual strength of the SiC/C/SiC minicomposites

The variations in the residual tensile strength of SiC/C/SiC minicomposites as a function of time under various stress levels at different temperatures, calculated from the model of residual strength by using the numerical values given in Tables 1 and 3, are shown in Fig. 13. It clearly appears from the figure that, as the oxidation time increases, the residual strength decreases and the rate of decrease of σ_{uts} increases rapidly. This is mainly due to the rapid consumption of carbon interface, which leads to the fact that the load-bearing mode changes from external load borne together by fibers, interface and matrix to by fibers alone [9]. Finally, the residual strength tends to stabilize at about 390 MPa. When the carbon interface is consumed by oxidation completely, the residual strength of the composite mainly reflects the properties of the SiC fibers, which will decrease slowly with the increase in oxidation time. Furthermore, the higher the temperature is, the rapider the rate of consumption of carbon interface is and the faster the degradation rate of residual strength is.

The variations in the residual tensile strength of SiC/C/SiC minicomposites versus time under various tensile stress levels (80–200 MPa) at 900 °C are shown in Fig. 14.

As expected, the decrease rate of the residual strength of the composite increases with the increase in tensile strength level at the same time and temperature. Because, as already mentioned above, the larger the tensile stress level is, the more matrix cracks appears and the wider the matrix crack is, which leads to more oxygen entering the interior of the composite to react with interface and fibers and accelerates the degradation of the properties of the composites.

The residual tensile strength of SiC/C/SiC minicomposites in stressed oxidizing environments (dry air) and the residual tensile strength of SiC/C/SiC composites were calculated using the numerical parameters (Fig. 15) at various temperatures (1100–1300 °C). Then, the predicted results were compared with the experiment data measured by Xin Jing et al. [39], where the residual tensile strength at 1100 °C and 1300 °C was obtained by test and that at 1200 °C was obtained by fitting the experimental curve of residual tensile strength versus temperature (see Fig. 15).

Table 2 Interfacial oxidation parameters at 900 °C under different stress levels

Tensile stress (MPa)	80	120	160	200
Sealing time (min)	75	131	202	289
Carbon length consumed by oxidation (mm)	3.4	4.59	5.69	6.73

Table 3 Values of the parabolic rate constants and of the oxygen concentration exponents for SiC fibers and SiC CVI matrix for temperatures ranging from 900 to 1200 °C

Temperature (°C)	B_f^* (nm^2 min^{-1})	B_m^* (nm^2 min^{-1})	p_f	p_m	Ref.
900	5	58	0.5	0.9	[10]
1000	49	83	0.5	0.8	
1100	188	139	0.5	0.7	
1200	404	285	0.5	0.6	
1300	587	396	0.5	0.5	
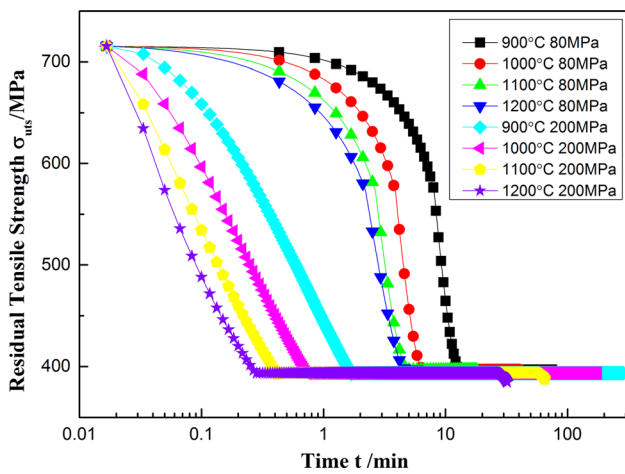
Figure 13 Variations in the residual tensile strength of SiC/C/SiC minicomposites as a function of time.

Figure 14 Variations in the residual tensile strength of SiC/C/SiC minicomposites versus time under various tensile stress levels (80–200 MPa) at 900 °C.

It clearly appears from Fig. 15 that the predicted results agree well with the experimental data and the error is less than 5%.

Furthermore, the predicted results of the present model were also compared with the calculated residual tensile strength based on the in situ fiber strength model [39] (see Fig. 15). It clearly appears from Fig. 15 that the present model is more accurate than the in situ fiber strength model, which indicates that the model presented in this paper is reasonable.

The model for predicting the residual strength of SiC/C/SiC minicomposites in stressed oxidizing environments can be used to foresee the influence of various test parameters, such as temperature, tensile stress level, oxygen partial pressure, the interface thickness, on the variation rate of the residual strength of minicomposite. In addition, the SiC/SiC composites are commonly used as the turbine disk stator of aeroengine hot sections, such as the turbine
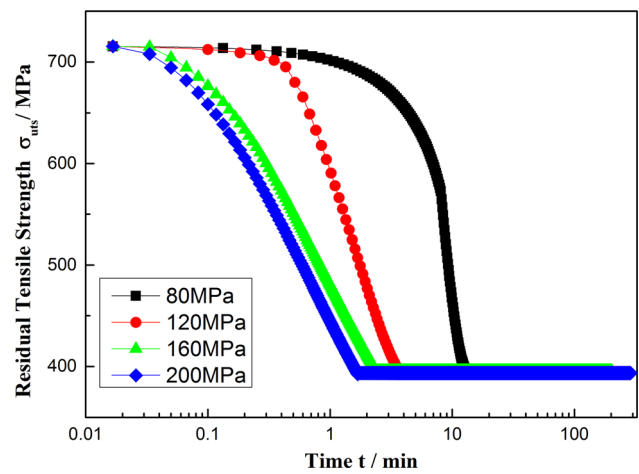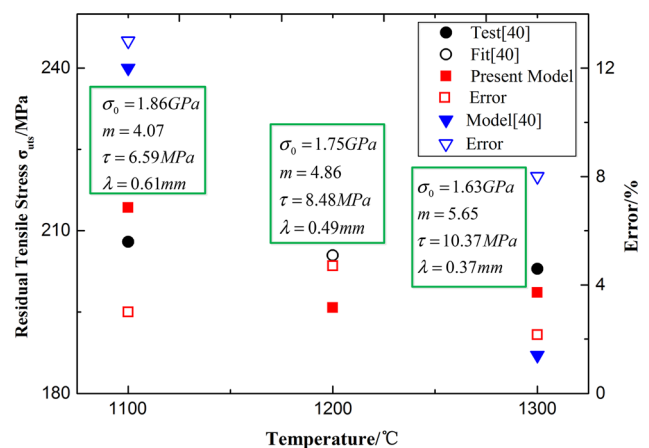

Figure 15 Predicted and experimental residual tensile strength of SiC/C/SiC composites versus temperature at 5 min.

blade, which are often exposed to a stressed oxidizing environment. The model developed in this paper

can be the basis of predicting the residual tensile strength and lifetime of these structures made by SiC/SiC composites.

Conclusions

A model, based on an oxidation kinetics model containing matrix cracks, has been developed to predict the residual tensile strength of SiC/C/SiC minicomposites in this paper. It takes into account the oxidation of carbon interface, SiC fibers and matrix, the change in the fiber stress distribution and the degradation of the strength of the fibers with time in stressed oxidizing environments. The sealing time of matrix cracks and annular pore resulting from the oxidation of SiC matrix and fibers is predicted, and the model shows that the matrix cracks are sealed firstly; thus, the internal oxidation of the composites is controlled by the sealing of matrix cracks. Furthermore, the tensile stress level cannot change the oxidation behavior of the composite and just change the amount of oxygen entering the annular pore by changing the matrix crack width. The probability of failure of the fibers is calculated based on the fiber stress distribution and the residual strength of the fibers. The matrix cracking model combining with the probability of failure of the fibers is used to simulate the residual strength of the composite. With oxidation time increasing, the residual strength of SiC/C/SiC minicomposites decreases and the rate of decrease of σ_{uts} increases rapidly. Finally, the residual strength tends to stabilize at a certain level before the sealing time.

It is worth to note that at present the proposed model is based on some simplifications of the real conditions. The following aspects are needed to be considered in the further study to improve the numerical model:

1. The simulations of residual strength of SiC/C/SiC minicomposites after the matrix cracks healing by silica are not taken into account in the present study. After the matrix cracks healing, the oxidation kinetics of carbon interface and SiC fibers will change. The path for oxygen entering into the interior of the minicomposite changes from matrix cracks to the pores in the matrix, which makes the oxidation scheme become more complicated. The dissolution of oxygen in the silica may also be taken into account. Thus, it would be necessary to improve the model to account for diffusion of oxygen in the pores and the dissolution of oxygen in the silica to predict the residual strength of SiC/C/SiC minicomposites after the matrix cracks healing by silica.

2. In the oxidation kinetics model, it is assumed that there is no consumption of oxygen at the bottom of matrix crack, where the number of moles of oxygen entering the bottom of matrix cracks equals that entering the two entrances of the annular pore. The SiC fibers will be oxidized to consume several moles of oxygen. However, for simplification of the oxidation kinetics model, the oxidation of SiC fibers at the bottom of matrix crack is not concerned at present. Therefore, it would be necessary to improve the oxidation kinetics model to account for the oxidation of SiC fibers at the bottom of matrix crack in the boundary conditions.

3. The assumption of one single straight fiber combining with a shell of dense SiC matrix with a constant thickness is proposed in the oxidation kinetics model. In fact, the fibers were randomly distributed and some fibers are in contact, which has an effect on the oxidation of the minicomposite. As an important supplement of our future work, the influence of contacting between fibers would be carefully studied.

Appendix

The Knudsen diffusion coefficient is usually given for a straight pore with a circular cross section in which the collisions of the molecules with the pore walls

occur equally in all radial directions. The situation is somewhat different in an annular pore and in a matrix crack since here the collisions of the molecules with the walls occur mainly in one single direction. Therefore, the Knudsen diffusion in an annular pore and in a matrix crack is easier than that taking place in a cylindrical pore with a diameter equal to the width of the annular pore or the width of the matrix crack. Thus, the Knudsen diffusion coefficient has to be calculated for the specific geometry of the pore resulting from the consumption of the carbon interface and of the matrix crack.

The deriving process of the Knudsen diffusion coefficient in an annular pore can be seen in Ref. [10], and the Knudsen diffusion coefficient D_K can be expressed as

$$D_K = \frac{4}{3} v_a \frac{S}{Pe} \tag{53}$$

where v_a is the mean velocity of the molecules, which can be written as

$$v_a = \left(\frac{8R_g T}{\pi M_{O_2}}\right) \tag{54}$$

where S is the area of the cross section of the pore and Pe is the perimeter of the cross section. It seems that D_K is itself proportional to S/Pe ratio charactering the cross section of the pore. For a matrix crack, the Knudsen diffusion coefficient can be rewritten as Eq. (9). Thus, D_K is a function of the matrix crack cross-sectional geometry.

References

[1] Udayakumar A, Ganesh AS, Raja S et al (2011) Effect of intermediate heat treatment on mechanical properties of SiC/SiC composites with BN interface prepared by ICVI. J Eur Ceram Soc 31:1145–1153

[2] Naslain R (2004) Design, preparation and properties of non-oxide CMCs for application in engines and nuclear reactors: an overview. Compos Sci Technol 64:155–170

[3] Ding D, Zhou W, Luo F et al (2012) Mechanical properties and oxidation resistance of SiCf/CVI-SiC composites with PIP-SiC interface. Ceram Int 38:3929–3934

[4] Chai Y, Zhou X, Zhang H (2017) Effect of oxidation treatment on KD-II SiC fiber-reinforced SiC composites. Ceram Int 43:9934–9940

[5] Droillard C, Lamon J (1996) Fracture toughness of 2-D woven SiC/SiC CVI-composites with multilayered interfaces. J Am Ceram Soc 79:849–858

[6] Naslain RR (1998) The design of the fibre-matrix interfacial zone in ceramic matrix composites. Compos A 29:1145–1155

[7] Naslain RR, Pailler RJF, Lamon JL (2010) Single-and multilayered interphases in SiC/SiC composites exposed to severe environmental conditions: an overview. Int J Appl Ceram Technol 7:263–275

[8] Mizuno M, Zhu S, Kagawa Y et al (1997) Stress, strain and elastic modulus behaviour of SiC-Fiber/SiC composites during creep and cyclic fatigue tests. Key Eng Mater 4:132–136

[9] Pailler F, Lamon J (2005) Micromechanics based model of fatigue/oxidation for ceramic matrix composites. Compos Sci Technol 65:369–374

[10] Filipuzzi L, Naslain R (2010) Oxidation mechanisms and kinetics of 1D-SiC/C/SiC composite materials: II, modeling. J Am Ceram Soc 77:467–480

[11] Singhal SC (1976) Oxidation kinetics of hot-pressed silicon carbide. J Mater Sci 11:1246–1253. https://doi.org/10.1007/BF00545142

[12] Frety N, Molins R, Boussuge M (1992) Oxidizing ageing effects on SiC–SiC composites. J Mater Sci 27:5084–5090. https://doi.org/10.1007/BF01105277

[13] Huger M, Fargeot D, Gault C (1994) Ultrasonic characterization of oxidation mechanisms in Nicalon/C/SiC composites. J Am Ceram Soc 77:2554–2560

[14] Filipuzzi L, Camus G, Naslain R et al (1994) Oxidation mechanisms and kinetics of 1D-SiC/C/SiC composite materials: I, an experimental approach. J Am Ceram Soc 77:459–466

[15] Fitzgerald K, Shepherd D (2018) Review of SiCf/SiC m, corrosion, erosion and erosion-corrosion in high temperature helium relevant to GFR conditions. J Nucl Mater 498:476–494

[16] Mohan A, Udayakumar A, Gandhi AS (2017) High temperature oxidation behaviour of CVD β-SiC seal coated SiCf/SiC composites in static dry air and combustion environment. Ceram Int 43:9472–9480

[17] Glime WH, Cawley JD (1998) Stress concentration due to fiber-matrix fusion in ceramic-matrix composites. J Am Ceram Soc 81:2597–2604

[18] Gogotsi YG, Yoshimura M (1995) Low-temperature oxidation, hydrothermal corrosion, and their effects on properties of SiC (Tyranno) fibers. J Am Ceram Soc 78:1439–1450

[19] Heredia FE, Mcnulty JC, Zok FW et al (1995) Oxidation embrittlement probe for ceramic-matrix composites. J Am Ceram Soc 78:2097–2100

[20] Morscher GN (1997) Tensile stress rupture of SiCf/SiCm minicomposites with carbon and boron nitride interfaces at elevated temperatures in air. J Am Ceram Soc 80:2029–2042

[21] Steyer TE, Zok FW, Walls DP (1998) Stress rupture of an enhanced Nicalon/silicon carbide composite at intermediate temperatures. J Am Ceram Soc 81:2140–2146

[22] Morscher GN (2010) Intermediate temperature stress rupture of woven SiC fiber, BN interphase, SiC matrix composites in air. J Am Ceram Soc 83:1441–1449

[23] Lin HT, Becher PF (1997) Effect of fiber coating on lifetime of Nicalon fiber-silicon carbide composites in air. Mater Sci Eng, A 231:143–150

[24] Ogbuji LUJT (1998) A pervasive mode of oxidative degradation in a SiC–SiC composite. J Am Ceram Soc 81:2777–2784

[25] Xu W, Zok FW, Mcmeeking RM et al (2014) Model of oxidation-induced fiber fracture in SiC/SiC composites. J Am Ceram Soc 97:3676–3683

[26] Casas L, Martínez-Esnaola JM (2003) Modelling the effect of oxidation on the creep behaviour of fibre-reinforced ceramic matrix composites. Acta Mater 51:3745–3757

[27] Yu G, Gao X, Chen Y et al (2018) Failure modeling of SiC/SiC mini-composites in air oxidizing environments. Appl Compos Mater 25:1441–1454

[28] Sun Z, Miao Y, Song Y (2012) Simulating and validating the stress-strain curve of the matrix cracking of ceramic matrix composite. J Aerosp Power 27:2056–2062

[29] Lamouroux F, Naslain R (1994) Kinetics and mechanisms of oxidation of 2D woven C/SiC composites: II, theoretical approach. J Am Ceram Soc 77:2049–2057

[30] Chateau C, Gélébart L, Bornert M et al (2014) Modeling of damage in unidirectional ceramic matrix composites and multi-scale experimental validation on third generation SiC/SiC minicomposites. J Mech Phys Solids 63:298–319

[31] Sun Z, Hong H, Niu X et al (2016) Simulation of mechanical behaviors of ceramic composites under stress-oxidation environment while considering the effect of matrix cracks. Appl Compos Mater 23:477–494

[32] Fuller EN, Schettler PD, Giddings JC (1966) New method for prediction of binary gas-phase diffusion coefficients. Ind Eng Chem 58:18–27

[33] Curtin WA (1991) Theory of mechanical properties of ceramic-matrix composites. J Am Ceram Soc 74:2837–2845

[34] Lara-Curzio E (1999) Analysis of oxidation-assisted stress-rupture of continuous fiber-reinforced ceramic matrix composites at intermediate temperatures. Compos A 30:549–554

[35] Lara-Curzio E, Ferber MK, Tortorelli PF (1996) Interface oxidation and stress-rupture of Nicalon/SiC CFCCs at intermediate temperatures. Key Eng Mater 127–131:1069–1082

[36] Lara-Curzio E (1997) Oxidation induced stress-rupture of fiber bundles. J Eng Mater Technol 120:105–109

[37] Curtin W, Ahn B, Takeda N (1998) Modeling brittle and tough stress–strain behavior in unidirectional ceramic matrix composites. Acta Mater 46:3409–3420

[38] Wilson M, Opila E (2016) A review of SiC fiber oxidation with a new study of Hi-Nicalon SiC fiber oxidation. Adv Eng Mater 18:1698–1709

[39] Xin J, Duoqi S, Xiaoguang Y et al (2015) Fiber strength measurement for KD-I(f)/SiC composites and correlation to tensile mechanical behavior at room and elevated temperatures. Ceram Int 41:299–307

[40] Sun Z, Shao H, Chen X et al (2016) Analysis of residual performance of UD-CMC in oxidation atmosphere based on a notch-like oxidation model. Appl Compos Mater 23:1079–1098

[41] Levy M (1962) Oxidation of pyrolytic graphite in air between 1250° and 1850°F. Ind Eng Chem Prod Res Dev 1:19–23

[42] Shoujun W (2006) Thermochemical environmental behaviors of 3D SiC/SiC composite. Ph.D. Dissertation, Northwestern Polytechnical University

Publisher's Note Springer Nature remains neutral with regard to jurisdictional claims in published maps and institutional affiliations.